Physics of the Solid State, 2024, Vol. 66, No. 10

03,05

Formation of ferromagnetic semiconductor GaMnAs by ion implantation: comparison of different types of annealing

© O.V. Vikhrova[1], Yu.A. Danilov[1], Yu.A. Dydin[1], A.V. Zdoroveyshchev[1], I.L. Kalentyeva[1], A.V. Kydrin[1], R.N. Kryukov[1], A.V. Nezhdanov[1], A.E. Parafin[2], M.K. Tapero[3,4], M.P. Temiryazeva[5], A.G. Temiryazev[5], A.A. Yakovleva[1]

[1] Lobachevsky State University of Nizhny Novgorod,
Nizhny Novgorod, Russia
[2] Institute for Physics of Microstructures, Russian Academy of Sciences,
Nizhny Novgorod, Russia
[3] MISIS University of Science and technology,
Moscow, Russia
[4] Prokhorov Institute of General Physics, Russian Academy of Sciences,
Moscow, Russia
[5] Fryazino Branch of Kotelnikov Institute of Radio Engineering and Electronics, Russian Academy of Sciences,
Fryazino, Moscow Region, Russia

E-mail: vikhrova@nifti.unn.ru

Received July 16, 2024
Revised September 26, 2024
Accepted September 28, 2024

The preparation of the ferromagnetic semiconductor GaMnAs by ion implantation and three types of annealing is considered: rapid thermal, pulsed laser, and combined annealing (a combination of rapid thermal and pulsed laser annealing). Rapid thermal annealing contributed to the improvement of crystallinity and the formation of clusters (including ferromagnetic ones at room temperature), and subsequent exposure to laser radiation led to their modification. When studying the structural, galvanomagnetic and magneto-optical properties, the formation of two ferromagnetic phases, differing in Curie temperature, was revealed in GaMnAs layers.

Keywords: ion implantation, rapid thermal annealing, pulsed laser annealing, two-phase ferromagnetic semiconductor.

DOI: 10.61011/PSS.2024.10.59620.195

1. Introduction

It is assumed that ferromagnetic properties of semiconductor $Ga_{1-x}Mn_xAs$ appear as a result of exchange interaction of atoms Mn through free charge carriers (holes), and an increase in concentration of introduced impurity shall result in Curie temperature increasing [1]. Mn concentration increasing above common 5−7% is difficult due to excess manganese embedding in interstitial positions (where interstitial atoms Mn_I are double donors) and formation of clusters of second phase (as a rule, MnAs). The highest Curie temperature $T_C = 191$ K for GaMnAs is achieved when Mn content reaches $x = 20\%$ during low-temperature ($T_g = 200°C$) molecular-beam epitaxy and use of low-temperature (140°C) long-term (for 16 h) annealing [2] to reduce concentration of Mn_I. Note that only 10.1% of Mn atoms of 20% are magnetoactive; destiny of rest 9.9% is unknown [2].

The method of implantation of Mn ions into GaAs provides considerable freedom in choice of concentration of doping atoms by varying the irradiation fluence. But at that there is need in annealing of the radiation faults formed during implantation and in impurity activation. As a rule, after the ion implantation (II) one of two annealing types is used: thermal high-temperature (at $T_a \approx 700-800°C$) or pulse laser annealing (generally by nanosecond pulse of excimer laser).

Rapid (generally for 10−30 s) thermal annealing (RTA), widely used currently in semiconductor technology, ensures annealing of GaAs samples in inert gas flow. It is known from [3] that after implantation of large ($\geq 10^{16}\,cm^{-2}$) fluences of Mn ions the impurity activation in GaAs occurs as result of RTA at temperature of 700−800°C, but at that the degree of activation (ratio sheet concentration of holes to ions fluence) does not exceed 0.3%. This means that the residual part of implanted Mn atoms is in electrically inactive state. In [3,4] it is shown that during RTA as a result of exceedance by concentration of Mn atoms of the limit of equilibrium solid-state solubility in GaAs some precipitates are formed, they are ferromagnetic at room temperature. Significant morphologic changes in form of surface clusters of GaMn type and embedded MnAs clusters that make difficult the use of II + RTA process in technology of spintronic devices [4].

The pulse laser annealing (PLA) was previously suggested to exclude the process of clusters formation in GaAs by fast heating of the layer, irradiated by Mn ions, at nanosecond powerful laser pulse and movement of front of recrystallization to surface with speed up to 10 m/s at cooling [5]. It is shown in [6] that PLA after implantation

of Mn ions into GaAs provides a single-phase ferromagnetic semiconductor with Curie temperature up to 110 K.

In present paper, unlike previous publications, the comparative studies of RTA and PLA are performed on GaAs samples obtained by implantation of Mn ions under same technological conditions. In addition, the properties of GaMnAs obtained in a combined annealing process, where after ion implantation, the RTA process is first performed, and then the PLA process is performed on the same sample, were studied for the first time. In addition, the properties of GaMnAs obtained in a combined annealing process, where after ion implantation, the RTA process is first performed, and then the PLA process is performed on the same sample, were studied for the first time.

2. Experimental procedure

Samples of GaMnAs layers were studied, they are part of single-crystal wafer i-GaAs (001) 350–400 μm thick, obtained by implantation of manganese ions and further annealing. For Mn ions implantation we used accelerator „Raduga-3M“ [7] with source of ions based on vacuum-arc discharge (initial material was wafer of metallic pure manganese). Features of this accelerator operation are absence of mass separation and presence in the ion beam of different charge fractions. Accelerating voltage in accelerator was 30 or 80 kV. The experimentally obtained distribution by charge states at typical parameters of vacuum arc discharge are provided for Mn in [8]. Distributions by charge states of manganese ions looks as follows: part of singly charged Mn^{+} is 49%, amount of Mn^{2+} and Mn^{3+} reaches 50 and 1% respectively.

Fluence of implanted ions varied from $2 \cdot 10^{16}$ to $5 \cdot 10^{16}\,cm^{-2}$. Under specified conditions of implantation the concentration of impurity ions in GaAs regions irradiated by ions in maximum can reach 8–10 at.%. Thickness of layer modified by the ion implantation, as per evaluations made by program SRIM, can be $\sim$ 150–200 nm.

RTA of ion-implanted GaAs was performed in unit JetFirst-100 in flow of high pure argon at temperature 750°C for 15 s. The substrate was wafer of low doped Si, and GaAs samples were loaded by work side bottom to prevent arsenic evaporation.

Annealing by single pulse of eximer KrF-laser LPX-200 (pulse width 30 ns, wavelength of laser radiation 248 nm) is made with energy density 400 mJ/cm^2.

Part of structures was subjected to combined procedure comprising two stages: initially RTA was performed, then on same samples PLA was performed under above specified conditions.

Structural properties were studied by Raman scattering (RS) spectra using unit NTEGRA Spectra. For radiation exciting the laser with wavelength 473 nm was used, its radiation was focused by lens 100× with aperture NA = 0.9. Laser radiation power was monitored using 11PD100-Si (Standa Ltd) silicon photodetector, and was equal to 0.5 mW. RS spectra were studied in geometry of back scattering in frequency range 50–900 cm^{-1} with resolution 0.7 cm^{-1}. The exposure time during measurements was 120 s.

Microstructure of samples annealed by different methods was studied using method of transmission electron microscopy (TEM) using microscope JEM-2100 with thermionic cathode LaB_6 at accelerating voltage 200 kV. The overview images were taken at magnification of 20 000–40 000. To study fine structure details the method of high-resolution transmission electron microscopy was used at magnification of 250 000–500 000. To obtain the microdiffraction image of region comprising manganese enriched inclusion the selector diaphragm with diameter 100 nm was used. Distribution of Ga, Mn and As atoms through thickness of GaMnAs layer was analyzed using method of energy-dispersive X-ray spectroscopy (EDX) using attachment Oxford Instruments. EDX-spectrum was obtained using converging electron beam from area with diameter of 5 nm. Sensitivity of used equipment for the element composition determination of studied structures was about 1 at.%.

The obtained TEM study results are analyzed using free accessed programs. In particular, the theoretical analysis was performed using program DigitalMicrograph v.3.0 [9], reference data on interplanar spacing obtained using program PTCLab [10], and reference data from crystallographic data base [11]. The Fourier transforms of high-resolution transmission microscopy are prepared using the mathematical tool built in program DigitalMicrograph v.3.0.

The surface morphology and domain structure of initial and irradiated samples were studied by methods of atomic-force microscopy and magnetic-force microscopy (AFM and MFM) using atomic-force microscope Smart-SPM (AIST-NT). Distributions of surface potential of annealed samples were studied using method known as Kelvin probe forced microscopy (KPFM). Technical implementation of KPFM has many variations, in our case two-pass method with registration of force gradient of electrostatic interaction at second pass was used [12]. At that the probe continuously (both in first pass, and second pass) oscillates at frequency close to the resonance frequency (about 100 kHz). In semi-contact mode in first pass the surface profile is measured, in second pass the probe is lifted and moves repeating the sample relief. At that in the second pass between the probe and sample the AC voltage is applied with relatively low frequency $f \approx 1$ kHz and DC bias voltage U. Presence of electrostatic interaction between the probe and sample results in that under action of force gradient the resonance frequency of probe changes. This affects the phase of its oscillations. Phase change will have harmonic at frequency f upon presence of potential difference between the probe and sample. Selecting value U such that this response is equal to zero, we can measure this potential difference and plot during scanning the map of its distribution over surface. As potential difference depends on difference of work functions of materials, this method is frequently used to visualize the foreign inclusions on surface.

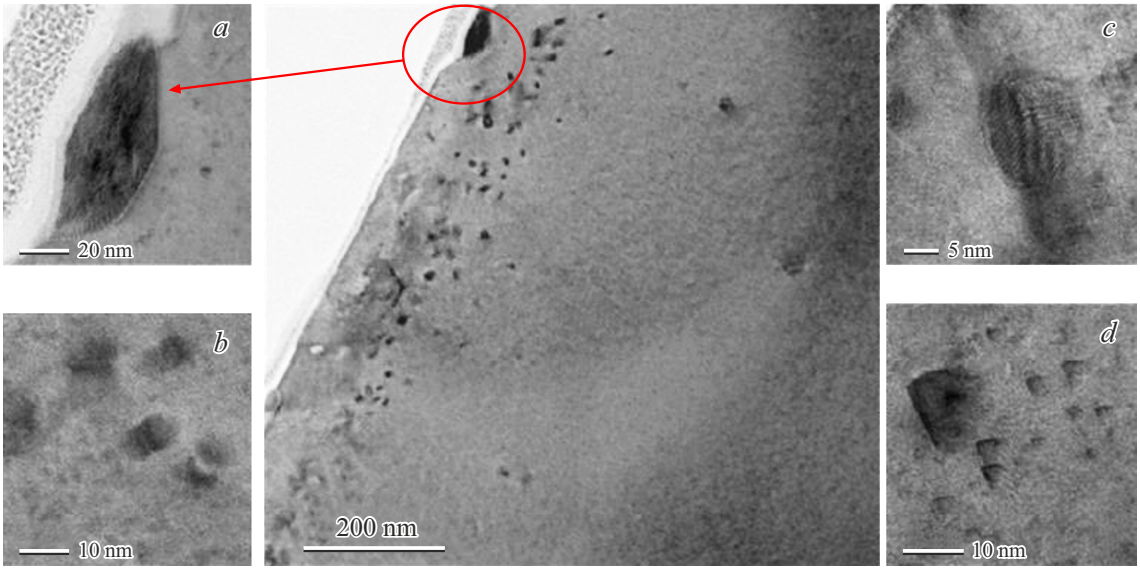

Figure 1. TEM-image of cross-section of GaMnAs layer obtained by Mn ions implantation at accelerating voltage of 80 kV with fluence $5 \cdot 10^{16}\,\mathrm{cm}^{-2}$ and further RTA. Fragment (a) is enlarged image of located near surface cluster of another crystal phase. Fragments (b) and (c) are images of clusters at depth about 150 nm, and fragment (d) demonstrates tetrahedral stacking faults [14].

Study of galvanomagnetic properties of annealed samples and magnetic circular dichroism (MCD) in spectrum range 1.15–2.5 eV for the geometry of reflection of circularly polarized light from the surface of the structures, was carried out using a closed-cycle helium cryostat with a magnetic field sweep within range ±3600 Oe at temperatures of 10 to 300 K. The magnetic field in experiments was applied perpendicular to sample surface.

3. Study results

3.1. Rapid thermal annealing

According to studies performed by transmission electron microscopy RTA under selected conditions restores crystallinity of layer irradiated by manganese ions, and results in significant decrease of number of radiation-induced faults. Also at RTA Mn doping is performed to concentrations not exceeding limit of equilibrium solubility. Limit solubility of manganese in GaAs lattice, determined from diagram of state of system Mn–GaAs, was $\sim 8 \cdot 10^{19}\,\mathrm{cm}^{-3}$ [13]. Excess Mn forms inclusions of second phase (most probably with Curie temperature above room temperature). The clusters formation is confirmed by TEM results. Figure 1 shows image of cross-section of GaMnAs layer obtained by Mn ions implantation at accelerating voltage of 80 kV with fluence $5 \cdot 10^{16}\,\mathrm{cm}^{-2}$ and further RTA. We see that thickness of the obtained GaMnAs layer is about 150 nm. At that several types of clusters (fragments a–c) and fault regions (fragment Figure 1, d) are observed. Large (size over 100×50 nm) clusters (inclusions) of first type (Figure 1, a) are located at surface of GaMnAs layer and have crystalline structure that differs from matrix. As per obtained data of energy-dispersive analysis these clusters comprise manganese, gallium and arsenic (content of Mn $\sim$ 26 at.%, Ga and As 35 and 39 at.%, respectively).

Inclusions of other type (Figure 1, b), prevailing at depth about 130–150 nm, demonstrate contrast of „coffee bean" type [14,15]. Size of these clusters varies from 5 to 10 nm. In many cases observation of particles that give such contrast allows to assume that they are coherently built into matrix [15]. On the contrary, the clusters of quasispherical shape with size about 15–20 nm (Figure 1, c) demonstrate contrast of moire [16], as they have crystalline structure that differs from the base material.

Figure 1, d demonstrates the defects staying after thermal annealing, in literature they were previously described for GaAs irradiated by silicon ions and identified as tetrahedral stacking faults [17]. Their size varies from 2 to 10–15 nm, at that most large of them can include precipitate indicating the moire contrast (Figure 1, d).

Probably, in such way regions are formed that correspond to clusters of hexagonal (α) MnAs (Figure 2, a). Exact phase composition of clusters can be discussed due to calculations of Fourier transform (Figure 2, b), obtained from direct image of cluster, where black circles mark reflexes corresponding to GaAs, red circles — reflexes α-MnAs.

Changes in phase composition of samples were characterized by study of surface potential distribution using KPFM and MFM. Figure 3 shows AFM-, MFM-images of surface and image of surface obtained in Kelvin-mode of GaMnAs layer formed by Mn ions implantation at accelerating voltage 80 kV with fluence $5 \cdot 10^{16}\,\mathrm{cm}^{-2}$ and further RTA. The observed contrast in image, obtained in Kelvin-mode, is due to difference in work functions of near-surface large clusters and matrix (probably, semi-metallic particles and

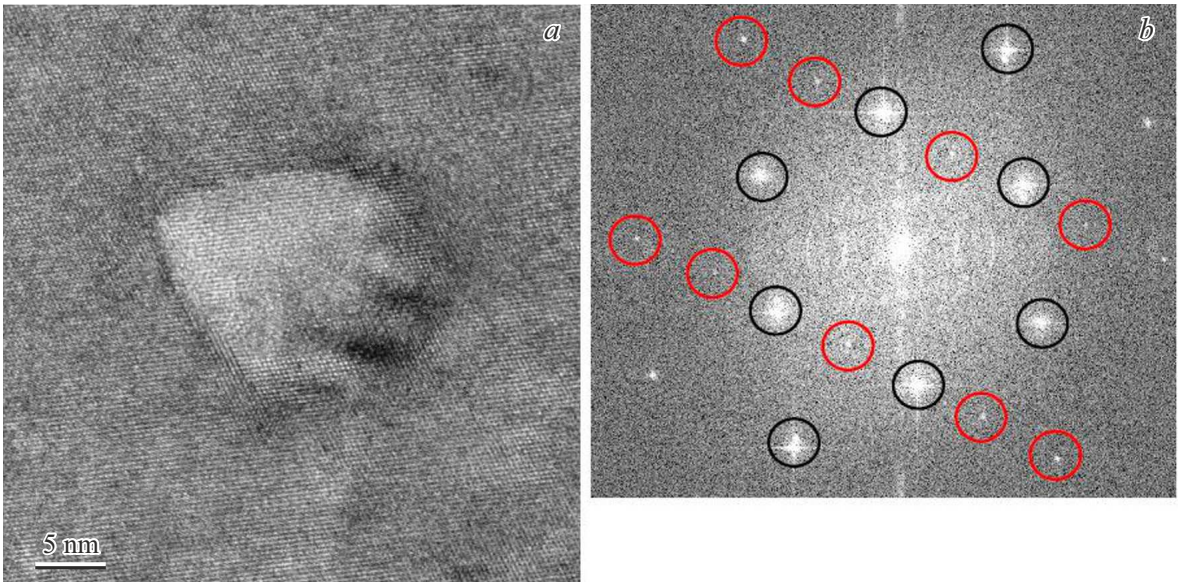

Figure 2. TEM-image with high resolution of cross section of GaMnAs, obtained by Mn ions implantation at accelerating voltage of 80 kV with fluence $5 \cdot 10^{16}\,\mathrm{cm}^{-2}$ and further RTA: *a*) TEM-image of cluster, *b*) calculated Fourier image (black circles mark reflexes corresponding to GaAs, red circles — reflexes α-MnAs).

semiconductor). MFM-image shows that part of these inclusions forms magnetic contrast, i.e. has ferromagnetic properties at room temperature.

Restoration of crystalline structure of GaMnAs samples manufactured using implantation and RTA is confirmed by study of RS spectra (Figure 4, spectrum *1*). Spectra comprise intense narrow peak in region of longitudinal optical (LO) mode ($291.2\,\mathrm{cm}^{-1}$) and weak peak for transverse optical (TO) mode ($267.4\,\mathrm{cm}^{-1}$). Presence of TO-mode is associated with small violations of geometry of light back scattering and/or deviation of wafer orientation from plane (100). Position of TO- and LO-modes within measurement error limits corresponds to their position for single-crystal GaAs.

Let's consider electrical properties of GaAs samples irradiated by Mn ions. Sample without annealing (implantation mode — 30 kV, fluence $2 \cdot 10^{16}\,\mathrm{cm}^{-2}$) has following electrical parameters: layer resistance $R_s = 2.72 \cdot 10^5\,\Omega/\square$, *n*-type of conductivity, effective Hall mobility $\mu_{\mathrm{eff}} = 0.6\,\mathrm{cm}^2/(\mathrm{V} \cdot \mathrm{s})$, layer concentration of electrons $n_s = 3.89 \cdot 10^{13}\,\mathrm{cm}^{-2}$. It is evident that these properties are due to radiation disorders occurred during ion implantation, and low mobility of charge carriers is associated with hopping conductivity of electrons between defects.

RTA of samples irradiated by Mn ions results in impurity activation (conductivity of *p*-type appears). As can be seen from Table as a result of fast thermal annealing the layer resistance of samples becomes about $1000\,\Omega/\square$, layer concentration of holes p_s reaches $3 \cdot 10^{13}\,\mathrm{cm}^{-2}$, and their mobility μ_{eff} is higher $200\,\mathrm{cm}^2/(\mathrm{V} \cdot \mathrm{s})$, which confirms significant improvement of structure of GaMnAs layers.

3.2. Pulse laser annealing

Figure 5 shows electron-microscope image of GaMnAs layer obtained by Mn ions implantation at accelerating voltage 80 kV with fluence $5 \cdot 10^{16}\,\mathrm{cm}^{-2}$ and further PLA. We can see that PLA use to treat the GaAs irradiated by manganese facilitates the restoration of crystalline structure and formation of overlapping twinning faults. The distribution of manganese through depth obtained by the energy dispersive analysis method allows us to estimate the thickness of the obtained GaMnAs layer (insert in Figure 5), which is about 50?60 nm. It is also evident that Mn in layer is distributed inhomogeneously, its content decreases from ~ 16 at.% near surface to ~ 1 at.% at depth 50–60 nm. Comparison of element composition of Mn, Ga and As in each region of EDX execution ensures supposition of predominant replacement of gallium atoms by manganese atoms in GaAs crystal lattice.

Analysis of RS results obtained after PLA of GaMnAs samples and presented in Figure 4 (spectrum *2* in Figure 4, *a* and spectra decomposition to Lorentzians in Figure 4, *b*), shows presence of coupled phonon-plasmon mode (CPLP). Besides, as compared to case of thermally annealed samples (spectrum *1*) significant decrease in intensity of peaks of LO- and TO-modes is observed, as well as slight offset to region of lower frequencies and widening. Such behaviour is due to disordering characterized by weakening of bonds and deviations from translation symmetry, i.e. by effects occurred during formation of GaMnAs solid solution [18,19]. Reason of occurrence of intensive, offsetted to region of low frequencies (up to $261.5\,\mathrm{cm}^{-1}$) of CPLP-mode is amplification of phonon-plasmon interaction in GaMnAs layer due to significant increase in concentration

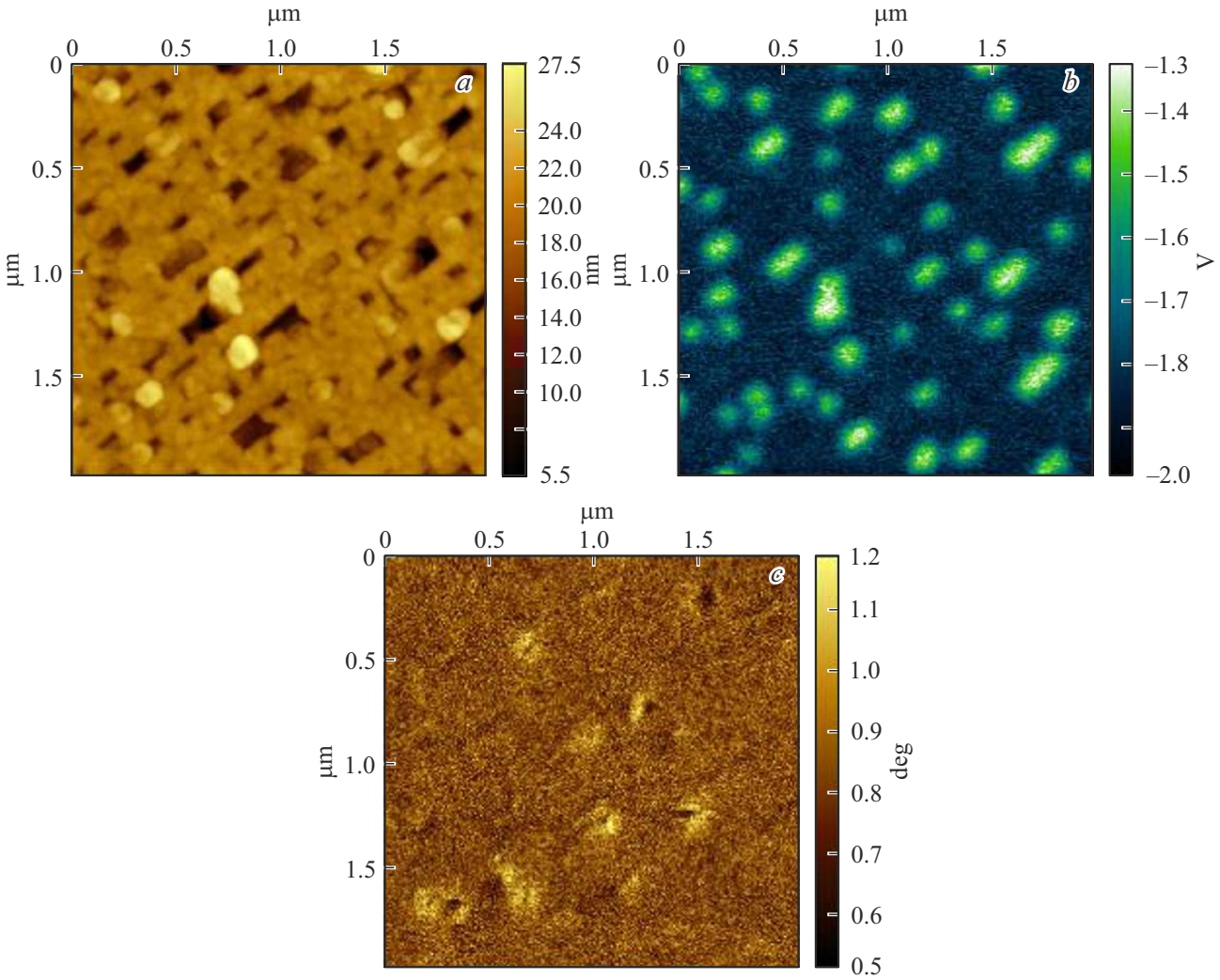

Figure 3. *a*) AFM-image of surface, *b*) image obtained in Kelvin-mode, and *c*) MFM-image of GaMnAs layer manufactured by Mn implantation at accelerating voltage 80 kV with fluence $5 \cdot 10^{16}$ cm^{-2} and further RTA.

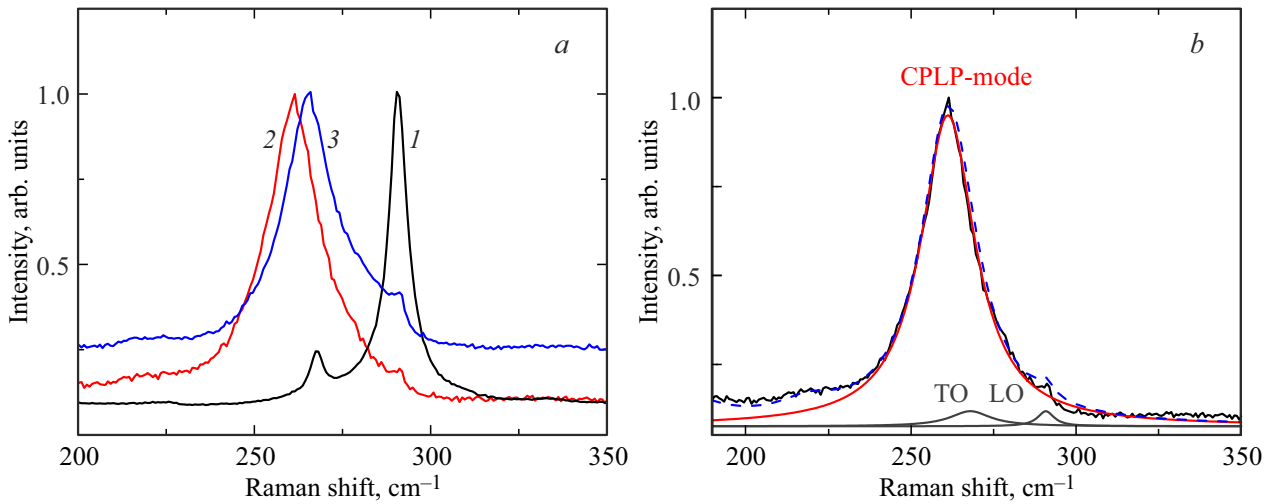

Figure 4. *a*) RS spectra of GaAs samples irradiated by Mn ions at accelerating voltage 80 kV with fluence $5 \cdot 10^{16}$ cm^{-2} after RTA (curve *1*), PLA (*2*) and combined annealing (*3*). *b*) RS spectrum and its decomposition to Lorentzians from GaAs sample subjected to pulse laser annealing with energy density 400 mJ/cm^2.

Electrical properties at room temperature of samples of GaMnAs layers obtained by ion implantation and further RTA, PLA and combined annealing (RTA and PLA with energy density $400\,\mathrm{mJ/cm^2}$). All samples have p-type of conductivity

Implantation mode	RTA 750°C/15s	PLA 400 mJ/cm^2	750°C/15s + PLA 400 mJ/cm^2
30 kV, $2 \cdot 10^{16}\,\mathrm{cm^{-2}}$	$R_s = 1050\,\Omega/\square$ $\mu_{\mathrm{eff}} = 215\,\mathrm{cm^2/(V \cdot s)}$ $p_s = 2.8 \cdot 10^{13}\,\mathrm{cm^{-2}}$	$R_s = 520\,\Omega/\square$ $\mu_{\mathrm{eff}} = 3.8\,\mathrm{cm^2/(V \cdot s)}$ $p_s = 3.15 \cdot 10^{15}\,\mathrm{cm^{-2}}$	$R_s = 710\,\Omega/\square$ $\mu_{\mathrm{eff}} = 120\,\mathrm{cm^2/(V \cdot s)}$ $p_s = 7.6 \cdot 10^{13}\,\mathrm{cm^{-2}}$
80 kV, $5 \cdot 10^{16}\,\mathrm{cm^{-2}}$	$R_s = 880\,\Omega/\square$ $\mu_{\mathrm{eff}} = 235\,\mathrm{cm^2/(V \cdot s)}$ $p_s = 3 \cdot 10^{13}\,\mathrm{cm^{-2}}$	$R_s = 460\,\Omega/\square$ $\mu_{\mathrm{eff}} = 4.8\,\mathrm{cm^2/(V \cdot s)}$ $p_s = 2.9 \cdot 10^{15}\,\mathrm{cm^{-2}}$	$R_s = 360\,\Omega/\square$ $\mu_{\mathrm{eff}} = 130\,\mathrm{cm^2/(V \cdot s)}$ $p_s = 1.4 \cdot 10^{14}\,\mathrm{cm^{-2}}$

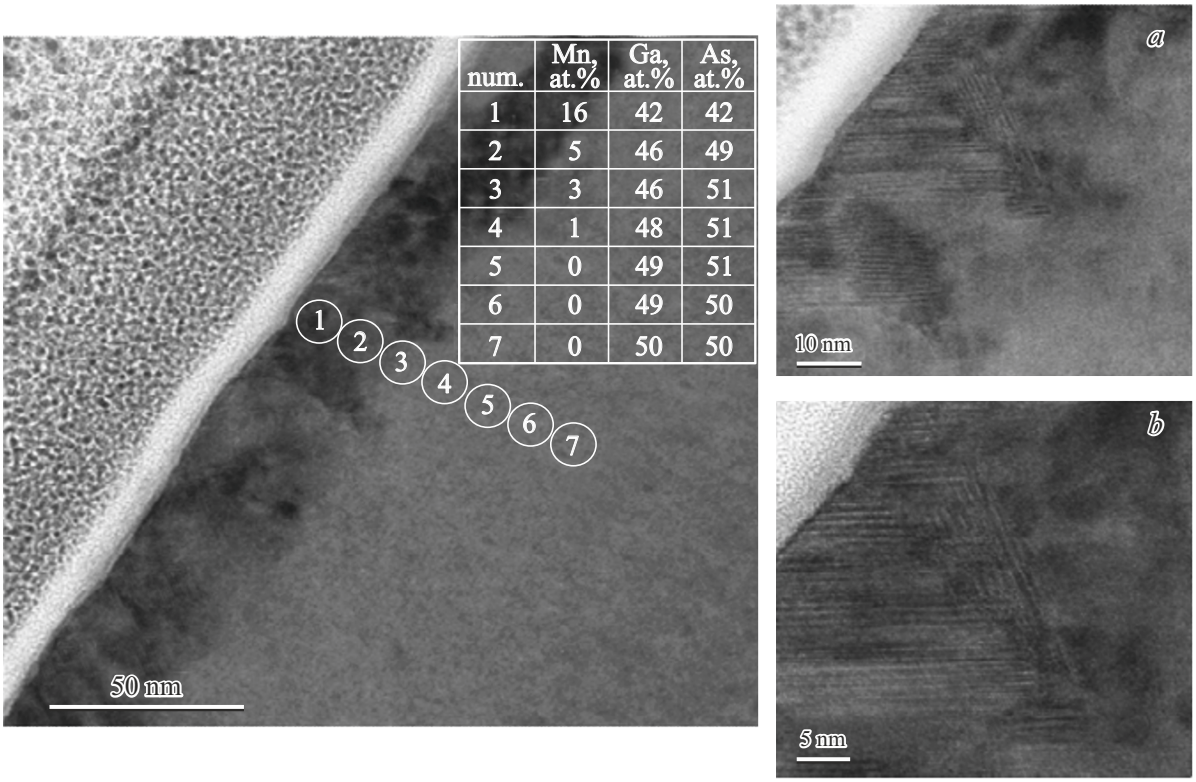

Figure 5. TEM-image of cross section of GaMnAs layer obtained by Mn ions implantation at accelerating voltage 80 kV with fluence $5 \cdot 10^{16}\,\mathrm{cm^{-2}}$ and further PLA. Table provides EDX data on content of Mn, Ga, As in marked points of GaMnAs layer. Fragments (a) and (b) — enlarged images of near-surface region of GaMnAs.

of charge carriers (holes) as result of pulse laser annealing. This is confirmed by presented in Table results of study of layer electrical parameters at room temperature: layer concentration of holes increases by 2 orders of magnitude as compared to RTA.

Figure 6 (curve *1*) presents layer resistance of GaMnAs sample obtained as per procedure II + PLA vs. measurement temperature. Position of resistance maximum, generally interpreted for ferromagnetic semiconductors as Curie temperature, is at $\sim 105\,\mathrm{K}$.

Figure 7, a presents magnetic field dependences of Hall resistance (R_{H}) of sample of type II + PLA at different measurement temperatures. Nonlinear dependences of Hall resistance with hysteresis loop are observed.

Therefore, for case of pulse laser annealing the type of dependences of Hall resistance on magnetic field corresponds to single-phase ferromagnetic semiconductor GaMnAs: with measurement temperature increasing the value of Hall saturation resistance steadily decreases (proportional to magnetization) as well as coercive field.

Figure 8, a shows the magnetic field dependences of magnetoresistance (MR) of sample subjected to PLA after ion implantation, for several measurement temperatures.

It is evident that MR is negative up to 80 K with sections of anisotropic MR at low temperatures. Generally, the galvanomagnetic properties of GaMnAs layers obtained during implantation at accelerator with source of Mn ions of vacuum arc discharge type with further PLA, are similar

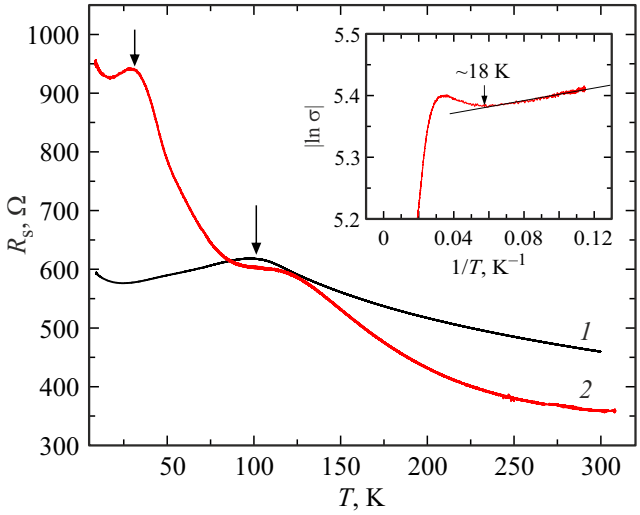

Figure 6. Temperature dependences of layer resistance of GaMnAs samples prepared by Mn ions implantation at accelerating voltage 80 kV (fluence $= 5 \cdot 10^{16}$ cm^{-2}) with further PLA (curve *1*) and with combined annealing (*2*). Arrows mark maximums complying to Curie temperature. The insert shows fragment of conductivity dependence on reciprocal temperature in logarithmic coordinates plotted from curve *2*.

to characteristics of layers obtained using implantation of monoenergetic Mn ions [20].

3.3. Combined annealing (RTA + PLA)

Results of TEM-studies of GaMnAs sample obtained by Mn ions implantation at accelerating voltage 80 kV with fluence $5 \cdot 10^{16}$ cm^{-2} and further combined annealing (RTA, then PLA), are shown in Figure 9.

As in case of only RTA use for post-implantation treatment, the thickness of obtained GaMnAs layer is about 150 nm, and clusters are observed (Figure 9, *a–c*). Here we can identify two main types of inclusions: first type — near-surface amorphous clusters with size $\sim 100 \times 50$ nm (fragment Figure 9, *a*), second type — inclusions (fragments Figure 9, *b* and *c*), located at depth about 130–150 nm, indicating contrast of „coffee bean" type [14,15]. According to contrast their boundaries are smeared, size varies approximately from 5 to 15–20 nm, their number is significant, and they overlap each other (Figure 9, *c*). Data of energy-dispersive analysis, shown in Figure, indicate predominance of manganese in near-surface amorphous inclusions (its portion reaches 92 at.%). For comparison, Mn content near surface in regions free of clusters is determined as 6 at.%.

RS data for GaMnAs sample obtained as result of combined annealing, also showed presence of bonded phonon-plasmon mode (Figure 4, *a*, curve *3*), as in case of PLA. We can only note that peak offset towards low values of wave number is lower for sample with combined annealing than for sample with PLA. This is in agreement with difference of layer concentrations of holes for combined and laser annealing (see Table). In case of sample obtained by implantation at accelerating voltage 80 kV with fluence of Mn ions $5 \cdot 10^{16}$ cm^{-2}, p_s value is $1.4 \cdot 10^{14}$ and $2.9 \cdot 10^{15}$ cm^{-2} for combined and laser annealing, respectively. Note significant increase in holes mobility (from ~ 4 to 120–130 cm^2/(V · s)) for combined annealing as compared to the laser annealing. As a result the layer resistance at 300 K in case of the combined annealing is $R_s = 360\,\Omega/\square$, this is significantly below the layer resistance $460\,\Omega/\square$ of sample annealed with laser.

Besides, the electrical properties of the layers obtained by combined annealing (see Table) significantly differ from properties of GaMnAs layers formed after RTA. First of

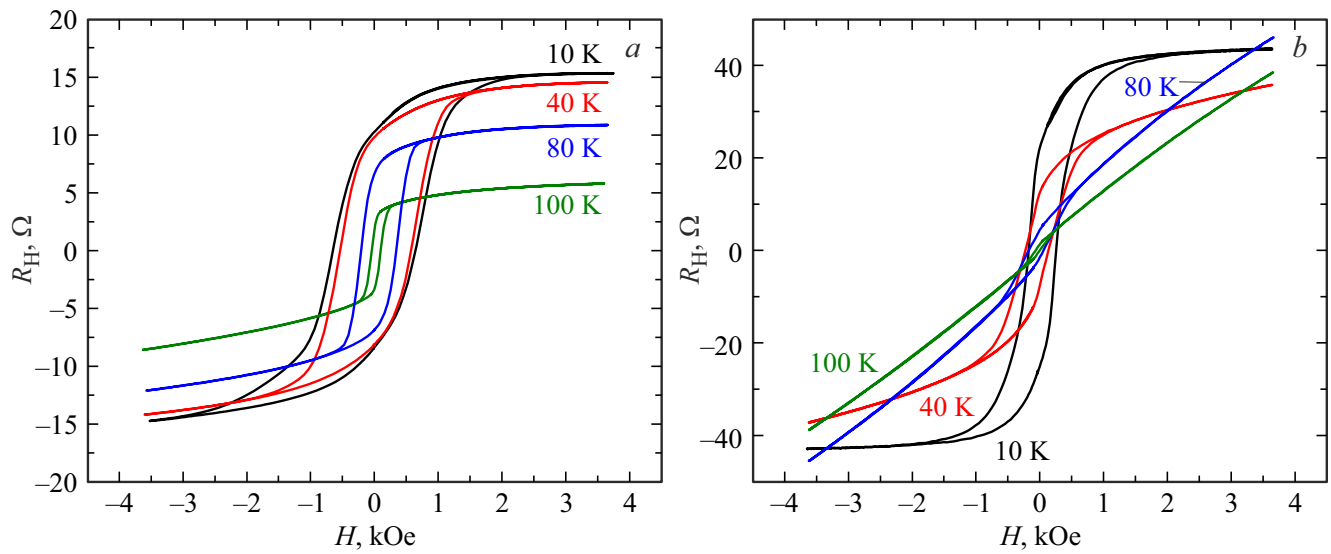

Figure 7. Magnetic field dependences of Hall resistance of GaMnAs layer Obtained by Mn ions implantation at accelerating voltage 80 kV (fluence $5 \cdot 10^{16}$ cm^{-2}) with further *a*) PLA or *b*) combined annealing.

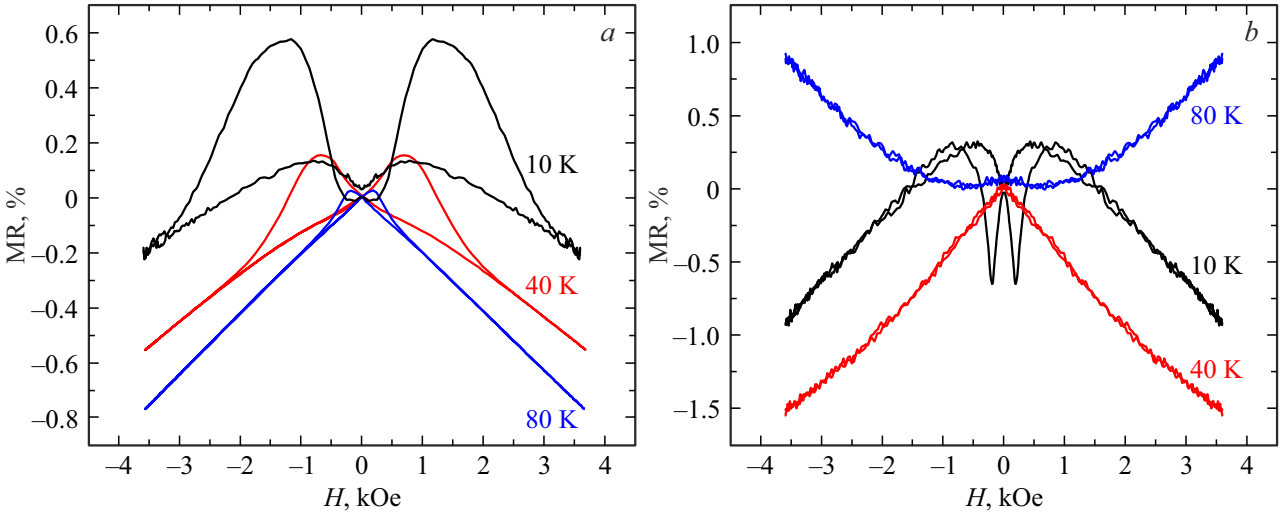

Figure 8. Magnetic field dependences of magnetoresistance of GaMnAs layer Obtained by Mn ions implantation at accelerating voltage 80 kV (fluence $5 \cdot 10^{16}\,\mathrm{cm}^{-2}$) with further *a*) PLA or *b*) combined annealing.

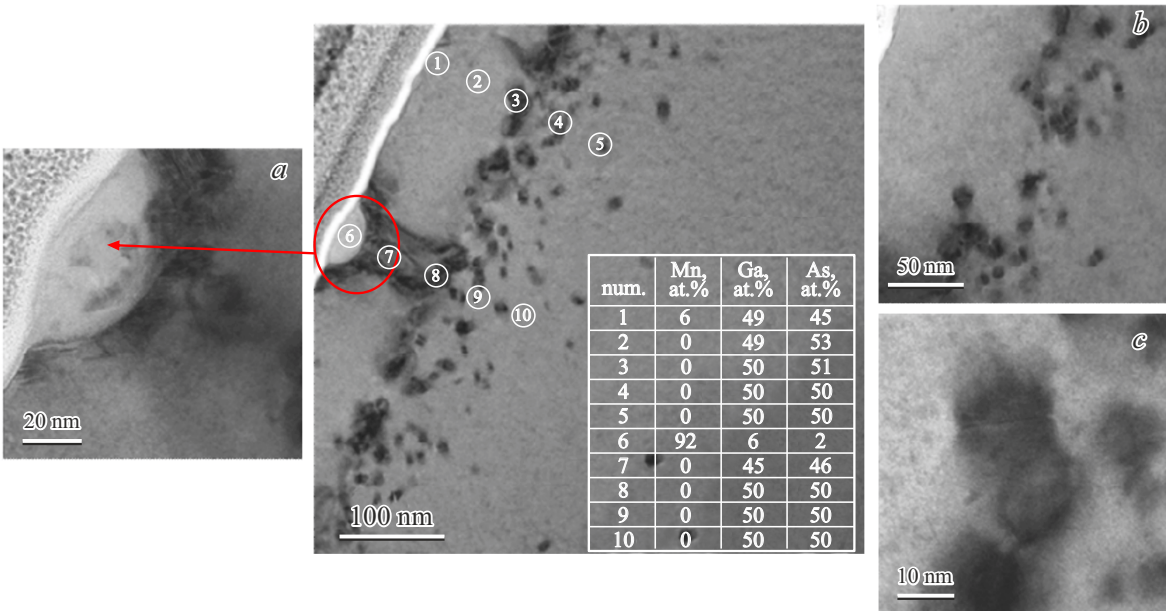

num.	Mn, at.%	Ga, at.%	As, at.%
1	6	49	45
2	0	49	53
3	0	50	51
4	0	50	50
5	0	50	50
6	92	6	2
7	0	45	46
8	0	50	50
9	0	50	50
10	0	50	50

Figure 9. TEM-image of cross section of GaMnAs layer obtained by Mn ions implantation at accelerating voltage 80 kV with fluence $5 \cdot 10^{16}\,\mathrm{cm}^{-2}$ and further combined annealing (RTA and then PLA). Table provides EDX data on content of Mn, Ga, As in marked points of GaMnAs layer. Fragment (*a*) is zoomed image of cluster located near surface. Fragments (*b*) and (*c*) — images of clusters at depth about 150 nm.

all, we pay attention to the fact that as a result of additional PLA, the layer concentration of holes increases by 3–4.5 times. At that their mobility somewhat decreases due to additional scattering as result of increased concentration of ionized acceptors Mn_{Ga}. We can expect that increase in concentration of Mn atoms in Ga nodes occurred as result of fault structure change of GaMnAs layer after additional exposure to laser irradiation.

Temperature dependence of layer resistance (Figure 6, curve *2*) of subjected to combined annealing GaMnAs sample (unlike the case on laser annealing only) contains two peaks. As maximums in dependences $R_s(T)$ of ferromagnetic materials are generally interpreted as increase in scattering of charge carriers near the phase transition ferromagnetic–paramagnetic, we can suppose that observed peaks can comply with two phase transitions with Curie temperature near 30–40 and 100 K respectively.

At that the nonlinear dependences of Hall resistance with hysteresis loop are observed, their view significantly change when temperature about 30 K is reached (Figure 7, *b*). At

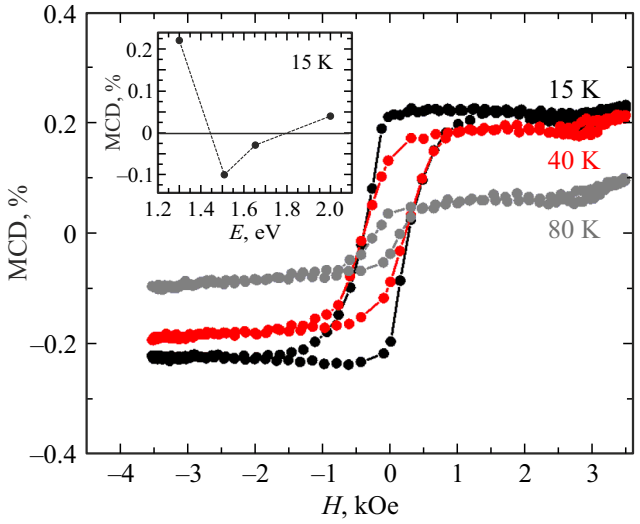

Figure 10. MCD-dependences for quantum energy 1.3 eV of GaAs sample, irradiated by Mn ions at accelerating voltage 80 kV with fluence $5 \cdot 10^{16}\,\mathrm{cm}^{-2}$ after combined annealing, for different measurement temperatures. The insert shows spectral dependence of MCD in field 3500 Oe at 15 K.

temperatures above 30–40 K contribution of normal (ordinary) Hall resistance increases, and further at temperature 120 K the magnetic field dependence of Hall resistance becomes linear.

Significant difference are observed also in MR behavior for two compared types of annealing (Figure 8). In case of GaMnAs sample subjected to PLA only negative MR is observed with positive regions of „ears" type corresponding to occurrence of anisotropic MR in ferromagnetic systems and kept until 80 K [21,22]. In case of combined annealing the sections of magnetic field dependences, which are determined by effect of anisotropic MR [23] comprising that resistance of ferromagnetic material depends on mutual orientation of magnetization direction of material and direction of flowing current, exist at temperature below 40 K only. Upon the measurement temperature increasing to 40 K MR becomes negative only, and for temperature of 60 K and higher the positive sections of MR(H) are registered in magnetic field over 1000–1500 Oe. The later is observed, probably, due to increase in contributions into GaMnAs layer conductivity of regions with higher mobility of holes.

For samples obtained by Mn ions implantation with further combined annealing the magnetic circular dichroism (MCD) was studied. The measurement results are shown in Figure 10. The magnetic field dependences of MCD signal of obtained samples are hysteresis. The hysteresis loop keeps until 80 K, this is in good agreement with Curie temperature obtained from the magnetic transport measurements. Spectral dependences of MCD are in agreement with the presented in literature data [24]. Signal appearance in region of quantum energies below band gap of GaAs is associated with formation of impurity bands in band gap.

4. Discussion of results

Let's start discussion and comparative analysis of presented results of use of three types of post-implantation (Mn) treatment of wafers of semi-insulating GaAs: RTA, PLA and their sequential combination.

Study by TEM methods showed significant difference of structural properties of obtained GaMnAs layers. In particular, after PLA the restoration of crystalline structure is observed with formation of twins and presence of manganese (increased towards surface) practically within complete layer within accuracy of detection (at least 1 at.%).

RTA use (under selected conditions) facilitates the crystalline structure restoration with appearance of tetrahedral stacking faults. RTA is accompanied by inclusions of three types, namely: near-surface large, enriched with manganese clusters, precipitates of semi-metal (hexagonal) MnAs and „buried" at distance 130–150 nm from surface coherent to basic crystalline lattice of inclusions with contrast of „coffee bean" type. Clusters located near the surface differ significantly from the semiconductor matrix in their electrical properties. In particular, they have work function which differs from the base material. Besides, from MFM-studies it follows that part of them are ferromagnetic at room temperature. At that we can assume that manganese content in semiconductor matrix is significantly below the threshold of detection by method of used energy-dispersive analysis, but not higher the limit equilibrium solubility of manganese in GaAs lattice (about $8 \cdot 10^{19}\,\mathrm{cm}^{-3}$ [13]). Electrical properties of the annealed samples at room temperature (see Table) confirm this supposition. Thus, in case of sample obtained by irradiation by Mn ions with accelerating voltage 80 kV and fluence $5 \cdot 10^{16}\,\mathrm{cm}^{-2}$, average volume concentration of holes reaches $\sim 2 \cdot 10^{18}\,\mathrm{cm}^{-3}$ (assuming thickness of GaMnAs layer equal to 150 nm), at that their mobility is $225\,\mathrm{cm}^2/(\mathrm{V} \cdot \mathrm{s})$. With measurement temperature decreasing to 80 and further to 10 K the significant (by several orders of magnitude) increase of layer resistance is observed.

PLA of sample previously subjected to RTA (i. e. combined annealing) results in disappearance of tetrahedral stacking faults and smearing of inclusion boundaries showing the „coffee bean" contrast. In this case, the large, manganese enriched clusters in surface are located much rarer, and are amorphous. Besides, manganese in amount of ~ 6 at.% was identified in the near-surface layer ~ 20 nm thick (Figure 9). The precipitates of α-MnAs having Curie temperature above the room temperature were not identified in studied region of sample. Magnetic contrast and contrast in Kelvin-mode at room temperature also were not observed for these samples. At same time the presented results of studies of temperature dependence of layer resistance (Figure 6, curve *2*), magnetic transport properties (Figure 7, *b* and Figure 8, *b*), magnetic field dependences of MCD and their analysis (Figure 10) showed existence of ferromagnetism with two Curie temperatures (about 30–40 and 120 K) in samples subjected to combined annealing.

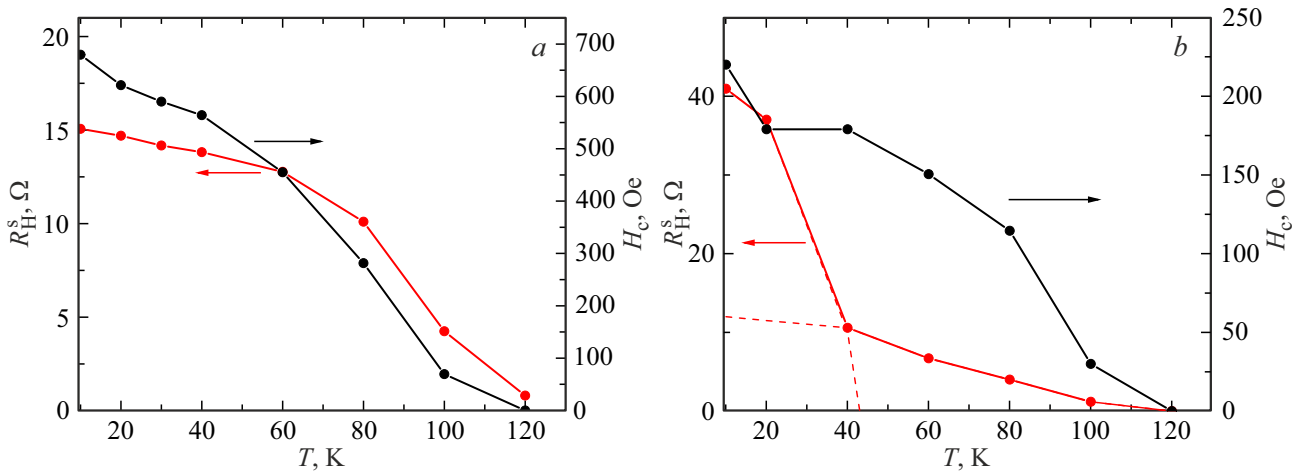

Figure 11. Temperature dependences of spontaneous Hall resistance and coercive field for GaMnAs layers obtained as result of Mn implantation at accelerating voltage 80 kV with fluence $5 \cdot 10^{16}\,\mathrm{cm}^{-2}$ and *a*) PLA and *b*) combined annealing.

The obtained logarithmic dependence of conductivity on reciprocal temperature (insert in Figure 6) can be approximated by the linear dependence in temperature range below 18–20 K, this confirms the prevailing of hopping conductivity in impurity band [25]. Such behaviour is possible in case when heavily doped by manganese degenerated GaMnAs layer is formed. The layer concentration of holes at room measurement temperature as result of PLA of sample previously subjected to RTA after ion implantation increases by about 4 times (see Table). This, firstly, means that part of earlier electrically inactive Mn atoms as a result of PLA enter the gallium nodes. This agrees with TEM-observation of GaMnAs structure after combined annealing (Figure 9). We can assume that formed after RTA Mn-containing clusters partially dissolve as a result of additional PLA.

Secondly, note that in spectrum of Raman scattering of sample subjected to combined annealing the intense phonon-plasmon mode appears (Figure 4, *a*). Type of RS spectrum in this case can be also used to evaluate the value of volume concentration of charge carriers. In particular, according to RS data presented in [26] for series of GaMnAs layers with different manganese content obtained by low-temperature MBE, we can assume that volume concentration of holes is our case shall be $\geq 10^{20}\,\mathrm{cm}^{-2}$. Thus, considering the layer concentration $p_s = 1.4 \cdot 10^{14}\,\mathrm{cm}^{-2}$ (for samples obtained under irradiation by Mn ions with accelerating voltage 80 kV and fluence $5 \cdot 10^{16}\,\mathrm{cm}^{-2}$), we can evaluate thickness of conductive near-surface layer ensuring basic contribution into RS spectrum as about 15–20 nm. Here we shall recall that according to wavelength of laser used in our case in RS spectroscopy, the depth of radiation penetration into GaAs is about 40 nm.

On other hand, holes mobility keeps high values ($\mu_{\mathrm{eff}} = 130\,\mathrm{cm}^2/(\mathrm{V}\cdot\mathrm{s})$) at room temperature as compared to case of only PLA use for post-implantation treatment ($\mu_{\mathrm{eff}} = 4.8\,\mathrm{cm}^2/(\mathrm{V}\cdot\mathrm{s})$). Besides, evaluations of mobility values from magnetic transport properties at temperatures of 100 to 140 K also showed large values — $\sim 1000-2000\,\mathrm{cm}^2/(\mathrm{V}\cdot\mathrm{s})$ for sample after combined annealing. This circumstance allows us to assume the formation of second conduction channel, where the carriers are scattered significantly less, located in a less doped and crystalline more perfect region of the structure. It is obvious that conductivity in this case is ensured via valence band.

At same time, ferromagnetic properties is kept at temperatures up to 100 K and inclusively in form of hysteresis presence on magnetic field dependence of Hall resistance (Figure 7, *b*).

At temperatures below Curie temperature in presented in Figure 7 dependences of Hall resistance on magnetic field makes basic contribution, and behaviour of Hall resistance can be approximately assumed proportional to magnetization. This ensures determination of the spontaneous Hall resistance $R_{\mathrm{H}}^{\mathrm{S}}$ which is proportional to spontaneous magnetization M_{S} and characterizes ferromagnetic ordering. Arrott's procedure [27] was applied comprising plotting the dependence $M^2(H/M)$ and finding M_{S} by extrapolation of its linear portion up to the intersection with the axis of ordinates. $R_{\mathrm{H}}^{\mathrm{S}}$ is calculated in the same way, but using dependences $R_{\mathrm{H}}^2(H/R_{\mathrm{H}})$. If linear extrapolation $R_{\mathrm{H}}^2(H/R_{\mathrm{H}})$ to $H = 0$ gives $(R_{\mathrm{H}}^{\mathrm{S}})^2 > 0$, then this means keeping of ferromagnetic ordering for this measurement temperature. If value $(R_{\mathrm{H}}^{\mathrm{S}})^2 < 0$, then the ferromagnetism is absent.

The obtained under Arrott procedure dependences of spontaneous Hall resistance on temperature $R_{\mathrm{H}}^{\mathrm{S}}(T)$ for GaMnAs layer, formed using the pulse laser or combined annealing are provided in Figure 11. Here change in coercive field (H_c) with measurement temperature is also shown.

Dependences $H_c(T)$ for both annealing methods look similarly. Dependences of spontaneous Hall resistance demonstrate different behaviour. It is obvious that for the case of combined annealing the dependence $R_{\mathrm{H}}^{\mathrm{S}}(T)$ can be approximated by two curves (Figure 11, *b*, dotted lines), and this ensures supposition of presence of two ferromagnetic phases with different Curie temperatures. At that even for temperature 80 K the positive MR is observed (Figure 8, *b*).

Such combination is not typical for ferromagnetic semiconductor and indicates that abnormal Hall effect observed in temperature range above 40 K is not associated with spin-orbital scattering of spin-polarized charge carriers. Then due to what the hysteresis dependence of Hall resistance is maintained? We can assume the effect on this process of clusters coherent to matrix and embedded in GaMnAs layer, as well as use for explanation of the mechanism of occurrence of abnormal Hall effect and its keeping until room temperatures in mixed-phase magnetic semiconductors, presented in detail in [28]. In particular, in this cited paper the model is suggested describing occurrence of abnormal Hall effect due to action of Lorentz force, occurred under effect of local magnetic fields formed by inclusions of second ferromagnetic phase, on charge carriers [28]. The hysteresis dependence of Hall resistance on external magnetic field in this case is due to heterogeneity of layer and by hysteresis dependence of magnetization of inclusions on external magnetic field. At that the semiconductor matrix itself, where these inclusions present, is paramagnetic.

Thus, the effects observed under selected conditions of combined annealing can be due to formation after RTA of the inclusions of three types, namely: near-surface large, enriched with manganese clusters, precipitates of semi-metal (hexagonal) MnAs and „buried“ at distance 130−150 nm from surface coherent to basic crystalline lattice of inclusions with contrast of „coffee bean“ type, and their further modification (completer or partial dissolving) during PLA. As a result in GaMnAs layer the interacting ferromagnetic regions of two types are formed, they differ by composition, level of doping with manganese, mechanism of occurrence of hysteresis dependence of Hall resistance (abnormal Hall) and temperature of phase transition ferromagnetic−paramagnetic. Conductivity in such GaMnAs layers is performed via the valence band and impurity band (in last case it can be hopping), at that the prevailing contribution of one of conductivity channels is determined by the measurement temperature. At lower temperatures (below 30−40 K the conductivity via impurity band prevails. With temperature increasing to values close to temperature 80−100 K and higher, until room temperature, the predominance of conductivity via valence band starts. This is confirmed by appropriate high values of mobility of charge carriers (holes).

5. Conclusion

The comparative studied presented in this paper of process of rapid thermal annealing, pulse laser annealing and their sequential combination (supposing initially RTA, and then on same sample — PLA) on GaAs samples obtained by Mn ions implantation under same conditions modes ensure the following conclusions:

— RTA facilitates the restoration of the sample crystallinity, doping to values of manganese impurity concentrations not higher than the equilibrium solubility limit (less than 1 at.%), and the formation of inclusions (including ferromagnetic ones at room temperature) of the second phase of three types;

— PLA results in restoration of crystal structure accompanied by the formation of twins, heavy doping with manganese (from ~ 16 at.% near surface to ~ 1 at.% at depth 50−60 nm) and formation of single-phase ferromagnetic semiconductor GaMnAs with Curie temperature ~ 105 K;

— combined process (RTA and then PLA) facilitates further improvement of crystalline property (in particular, tetrahedral stacking faults disappear), modification of second phase inclusions (their partial or complete dissolving) and formation of GaMnAs layer with two ferromagnetic phases that differ by composition, level of doping with manganese, mechanism of occurrence of hysteresis dependence of Hall resistance and temperature of phase transition ferromagnetic-paramagnetic.

Funding

The study was sponsored by the Russian Scientific Foundation (grant No. 23-29-00312). Measurements by methods of atomic- and magnetic force microscopy, and study of distribution of surface potential of annealed samples using the method known as Kelvin probe force microscopy, were obtained in Fryazino branch of Kotelnikov Radio Engineering and Electronics Instutute of RAS.

Conflict of interest

The authors declare that they have no conflict of interest.

References

[1] T. Dietl. Semicond. Sci. Technol. **17**, *4*, 377 (2002).
[2] L. Chen, S. Yan, P.F. Xu, J. Lu, W.Z. Wang, J.J. Deng, X. Qian, Y. Ji, J.H. Zhao. Appl. Phys. Lett. **95**, *18*, 182505 (2009).
[3] Yu.A. Danilov, A.V. Kruglov, E.A. Pitirimova, Yu.N. Drozdov, A.V. Murel, M. Behar, M.A.A. Pudenzi. Izv. RAN. Ser. fiz. **68**, *1*, 65 (2004). (in Russian).
[4] O.D.D. Couto Jr, M.J.S.P. Brasil, F. Iikawa, C. Giles, C. Adriano, J.R.R. Bortoleto, M.A.A. Pudenzi, H.R. Gutierrez, I. Danilov. Appl. Phys. Lett. **86**, *7*, 071906 (2005).
[5] M.A. Scarpulla, O.D. Dubon, K.M. Yu, O. Monteiro, M.R. Pillai, M.J. Aziz, M.C. Ridgway. Appl. Phys. Lett. **82**, *8*, 1251 (2003).
[6] S. Zhou. J. Phys. D **48**, *26*, 263001 (2015).
[7] A.I. Ryabchikov, S.V. Dektjarev, I.B. Stepanov. Rev. Sci. Instrum. **65**, *10*, 3126 (1994).
[8] I.G. Brown, X. Godechot. IEEE Trans. Plasma Sci. **19**, *5*, 713 (1991).
[9] Electronic source. https://www.gatan.com/products/tem-analysis/gatan-microscopy-suite-software
[10] Electronic source. https://www.iucr.org/resources/other-directories/software/ptclab
[11] Electronic source: http://www.crystallography.net
[12] T.E. Sukhanova, M.P. Temiryazeva, M.E. Vylegzhanina, S.V. Valueva, A.Ya. Volkov, A.A. Kutin, A.G. Temiryazev. AIP Conf. Proceed. **1748**, *1*, 020003 (2016).

[13] S.K. Kuznetsova. Neorg. mater. **11**, *5*, 950 (1975). (in Russian).
[14] M. Wu, E. Luna, J. Puustinen, M. Guina, A. Trampert. Nanotechnol. **25**, *20*, 205605 (2014).
[15] A. Maltsi, T. Niermann, T. Streckenbach, K. Tabelow, T. Koprucki. Opt. Quant. Electron. **52**, 257 (2020).
[16] M. Moreno, A. Trampert, B. Jenichen, L. Daweritz, K.H. Ploog. J. Appl. Phys. **92**, *8*, 4672 (2002).
[17] W.G. Opyd, J.F. Gibbons, A.J. Mardinly. Appl. Phys. Lett. **53**, *16*, 1515 (1988).
[18] W. Limmer, M. Glunk, S. Mascheck, A. Koeder, D. Klarer, W. Schoch, K. Thonke, R. Sauer, A. Waag. Phys. Rev. B **66**, *20*, 205209 (2002).
[19] M.J. Seong, S.H. Chun, H.M. Cheong, N. Samarth, A. Mascarenhas. Phys. Rev. B **66**, *3*, 033202 (2002).
[20] Yu.A. Danilov, Yu.A. Agafonov, V.I. Bachurin, V.A. Bykov, O.V. Vikhrova, V.I. Zinenko, I.L. Kalentyeva, A.V. Kudrin, A.V. Nezhdanov, A.E. Parafin, S.G. Simakin, P.A. Yunin, A.A. Yakovleva. Phys. Solid State **65**, *12*, 2138 (2023).
[21] M.A. Scarpulla, R. Farshchi, P.R. Stone, R.V. Chopdekar, K.M. Yu, Y. Suzuki, O.D. Dubon. J. Appl. Phys. **103**, *7*, 073913 (2008).
[22] A.V. Kudrin, O.V. Vikhrova, Yu.A. Danilov. Tech. Phys. Lett. *36*, *6*, 511 (2010).
[23] K.Y. Wang, K.W. Edmonds, R.P. Campion, L.X. Zhao, C.T. Foxon, B.L. Gallagher. Phys. Rev. B **72**, *8*, 085201 (2005).
[24] K. Ando, H. Saito, K.C. Agarwal, M.C. Debnath, V. Zayets. Phys. Rev. Lett. **100**, *6*, 067204 (2008).
[25] B.I. Shklovsky, A.L. Efros. Elektronnye svojstva legirovannykh poluprovodnikov. Nauka, M. (1979). 416 s. (in Russian).
[26] W. Limmer, M. Glunk, W. Schoch, A. Köder, R. Kling, R. Sauer, A. Waag. Physica E **13**, *2–4*, 589 (2002).
[27] A. Arrott. Phys. Rev. **108**, *6*, 1394 (1957).
[28] A.V. Kudrin, A.V. Shvetsov, Yu.A. Danilov, A.A. Timopheev, D.A. Pavlov, A.I. Bobrov, N.V. Malekhonova, N.A. Sobolev. Phys. Rev. B **90**, *2*, 024415 (2014).

Translated by I.Mazurov